

## MINERALOGY AND PETROLOGY OF LASER IRRADIATED CARBONACEOUS CHONDRITE MIGHEI.

T.V. Shingareva<sup>1</sup>, A.T. Basilevsky<sup>1</sup>, A.V. Fisenko<sup>1</sup>, L.F. Semjonova<sup>1</sup>, N.N. Korotaeva<sup>2</sup>; <sup>1</sup>Vernadsky Institute, RAS, Moscow, 119991, Russia, shingareva@geokhi.ru; <sup>2</sup>Moscow State University, Russia.

**Introduction:** For the last several years a number of laser irradiation experiments have been performed to simulate space weathering on the surface of the Moon and asteroids [e.g., 1-6]. Some researchers used nanosecond-pulse laser simulating effects of micrometeorite bombardment by particles of 1-10  $\mu\text{m}$  in diameter. Such treatment leads to formation of SMFe on the surface of irradiated samples [1-3]. We used a microsecond-pulsed laser irradiation which simulates micrometeorite bombardment by 30-50 $\mu\text{m}$  particles if their density is 2-3  $\text{g}/\text{cm}^3$  and velocity  $\sim 1-3$  km/s [4-6]. Such treatment leads to the melting of the treated material and consequent quenching of the melt [4].

The goal of this study is simulation of the mineralogical and petrological changes in the products of micrometeorite bombardment of carbonaceous chondrite material, the case when micrometeorites are relatively large. Carbonaceous chondrites are considered as representing materials of the C- and D-type asteroids and maybe Phobos [7]. In this study we irradiated the CM chondrite **Mighei**.

Table1.

	Mighei		Irradiated Mighei		
	Matrix	Bulk sample	Bulk melt	Ol	Meso stasis
SiO <sub>2</sub>	32.54	33.96	38.72	38.38	40.83
TiO <sub>2</sub>	b.d.	0.14	0.15	0.06	0.36
Al <sub>2</sub> O <sub>3</sub>	2.55	2.53	3.38	1.47	7.51
FeO	32.21	28.01	25.91	22.15	33.75
MnO	0.33	0.4	0.33	0.31	0.36
MgO	21.44	21.07	26.59	35.53	7.12
CaO	1.73	1.55	2.41	1.31	6.02
Na <sub>2</sub> O	0.56	1.24	0.64	0.26	0.51
K <sub>2</sub> O	b.d.	0.27	b.d.	b.d.	b.d.
Cr <sub>2</sub> O <sub>3</sub>	0.58	0.65	0.62	0.56	0.80
P <sub>2</sub> O <sub>5</sub>	0.29	0.39	b.d.	0.07	b.d.
SO <sub>3</sub>	5.81	7.68	0.43	0.08	1.23
CoO	n.d.	0.33	0.18	b.d.	0.33
NiO	1.87	1.79	b.d.	b.d.	b.d.
Sum.	99.42	100.01	99.38	100.18	98.81

**The starting material and experimental procedure.** The CM2 chondrite **Mighei** consists largely of fine-grained black matrix and of olivine-rich chondrules, olivine aggregates, carbonates and sulfides. The matrix consists of Fe-rich serpentine-tochilinite intergrowth intimately mixed with carbonaceous material [8]. The sample was ground and sieved to  $<40$   $\mu\text{m}$ . Chemical composition is presented in the Table1.

The experimental procedure by microsecond pulse laser irradiation under  $(2-4) \times 10^{-4}$  mm Hg

vacuum was performed at the same conditions as in experiments [4-6].

The irradiation of **Mighei** was accompanied by noticeable sputtering of the melted matter and the ten-fold gas pressure increase in the experiment chamber, both apparently due to the volatile release from the melting material. Due to electrostatic forces the powdered material formed agglomerate clots up to 1-2 mm in diameter. In some of them, the laser beam made holes of  $\sim 100$   $\mu\text{m}$  in diameter filled in with the melt. The laser treatment mostly resulted in the formation of spherical glassy droplets from 20  $\mu\text{m}$  to 100  $\mu\text{m}$  in diameter and their aggregates which were then sieved into several size fractions to study VIS-IR spectra of the experiment products (see the companion work [9]). The coarser fractions were used for SEM and microprobe studies.

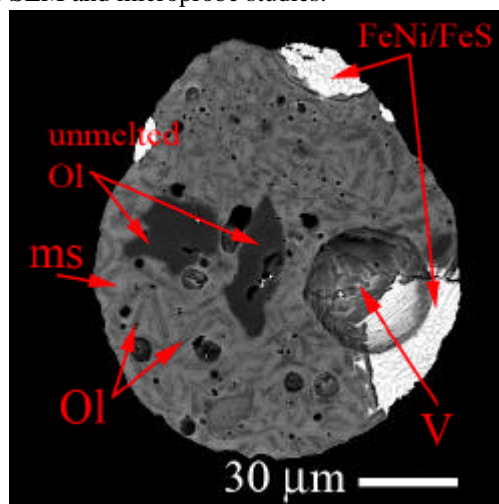


**Fig.1** BSE image of Mighei melt droplet: Ol – olivine, ms – mesostasis, V – vesicles.

**Mineralogy and petrology of experimental products.** Chemistry analyses and BSE imaging of altered samples were made at the Moscow State University Camebax SX 50 microprobe facility and SEM (CamScan 4 DV). It is seen on SEM images that the laser irradiation of **Mighei** did not lead to complete melting of all the irradiated matter: in some cases the melt contains inclusions of unmelted angular clasts of two compositional types of olivine (Fo<sub>99</sub> and Fo<sub>82</sub>). Apparently these two compositional types reflect the presence of two olivines in the initial sample: pure forsterite of the chondrules and more ferrous olivine presenting as single grains included in matrix. These clasts are 6-35  $\mu\text{m}$  in length and surrounded by thin ( $\sim 1-2$   $\mu\text{m}$ ) envelopes of olivine with more ferrous composition (Fo<sub>68</sub>).

The experiment products show two types of texture: intersertal and sometimes microporphritic. In general, the crystallization of the melt resulted in the

formation of compositionally zoned (with Fe-rich  $\sim 0.5\mu\text{m}$  rims) skeletal to filamentous olivine ( $\text{Fo}_{74}$ ) crystals (8 to 100  $\mu\text{m}$  long and 2 to 13  $\mu\text{m}$  wide) (fig.1). The olivine crystals are embedded in a Fe-rich (FeO 34%) glassy mesostasis. Also there are very fine (0.1-0.5 $\mu\text{m}$ ) Fe-rich opaque inclusions dispersed in the mesostasis (fig. 2). The melt contains gas bubbles from  $\sim 0.1$  to 70  $\mu\text{m}$  in diameter and metal/sulfide aggregates up to 60  $\mu\text{m}$  in diameters which include the large gas bubbles, too. The metal/sulfide inclusions are mostly concentrated in the external parts of the melt droplets, not as splashes on the droplet surface but being disseminated in the droplet groundmass. Comparing to the initial material the bulk melt composition is depleted in Fe, Ni, S and in Na (probably due to FeNi/troilite segregations and to vaporization) and proportionally enriched in all other components (Tab.1).

Table 2.

Treated sample	Initial mineralogy	Mineralogy of altered samples
Tsarev L5	Ol ( $\text{Fo}_{74}$ ), Opx, Cpx, Pl, gl, FeNi, FeS, $\text{FeCr}_2\text{O}_4$	Ol ( $\text{Fo}_{83}$ ), gl (23% FeO), FeNi, FeS
The mixture	Ol ( $\text{Fo}_{74}$ ), Opx, Cpx, Pl, gl, serpentine, kerite, calcite	Ol ( $\text{Fo}_{93}$ ), gl (18% FeO), FeNi, FeS
Mighei CM2	Serpentine, tochilinite, Ol ( $\text{Fo}_{99}$ , $\text{Fo}_{82}$ ), FeS, FeNi, $\text{FeCr}_2\text{O}_4$ , carbonaceous material, carbonates	Ol ( $\text{Fo}_{74}$ ), gl (34% FeO), FeNi, FeS

**Discussion and conclusions.** Laser treatment of **Mighei** concluded a series of our experiments with three types of samples: ordinary chondrite L5 **Tsarev**, carbonaceous chondrite CM2 **Mighei** and the artificial simulant of CM chondrite (**The mixture**) [5,6]. In these experiments laser pulse heating led to local melting, formation of the melt droplets and their subsequent cooling with partial crystallization. This resulted in formation of compositionally zoned (Fe-enriched rims) skeletal to filamentous Mg-olivine crystals cemented by Fe-rich glass (Table 2). The olivine composition is obviously dependent on the Mg/Fe ratio in the initial material. In all altered samples the glassy mesostasis had quasi-pyroxene composition and contains dispersed very fine (0.1 to 1 $\mu\text{m}$ ) Fe-rich opaque inclusions (fig. 2). Metal/sulfide phases segregated concentrating mostly in the outer parts of the melt droplets. Although not specially studied, the volatile components ( $\text{H}_2\text{O}$  of serpentine and chlorite and  $\text{CO}_2$  of calcite) have undoubtedly escaped from the melting products of **Mighei** and **The mixture**.

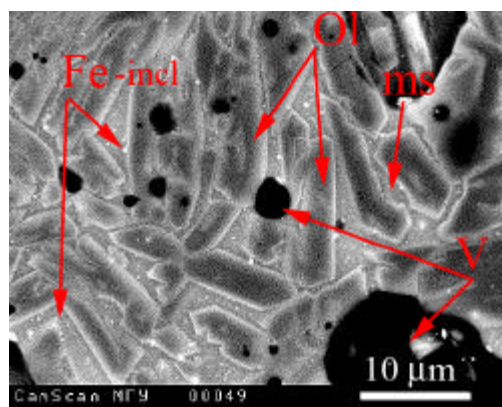


**Fig.2** BSE image of Mighei: Ol – olivine, ms – mesostasis, V – vesicles, Fe-incl. – Fe-rich fine inclusions.

In this study we modeled only part of the space weathering processes on the airless bodies, that one which is due to impacts of the high-velocity particles of tens microns in diameter. This process leads to the described above chemical and mineralogical changes and accumulation of Fe-rich submicron particles in the residual melt, which may be 'volume-correlated' SMFe [10], but this assumption must be verified in our future work. So in sense of chemistry and mineralogy the mature regolith on S-type asteroids (source of ordinary chondrites) and C+D-type asteroids (source of carbonaceous chondrites) and probably on Phobos is to be different comparing to the unweathered material [e.g., 11,12]. In particular, these changes has to be taken into account planning the Phobos-Grunt mission *in-situ* studies and the subsequent laboratory studies of the returned samples.

**Acknowledgment:** The work was supported by RFBR grant 02-05-65156.

**References:** [1] Yamada M. et al. (1999), *Earth Planets Space*, **51**, 1255-1265. [2] Sasaki S. et al. (2001), *Nature*, **410**, 555-557. [3] Hiroi T. & Sasaki S. (2002), *Meteor. Planet. Sci.*, **36**, 1587-1596. [4] Moroz L.V. et al. (1996), *Icarus*, **122**, 366-382. [5] Shingareva T.V. et al. (2003), *LPS XXXIV*, #1321. [6] Shingareva T.V. et al. (2003), Vernadsky/Brown Microsymposium 38, # MS086. [7] Pang K.D. et al. (1978), *Science*, **199**, N 4324, 64-66. [8] Zolensky M. & McSween H. (1988), In: *Meteorites and the early Solar System* Univ. of Arizona Press, Tucson, 114-143. [9] Moroz L. V. et al. (2004), *LPS XXXV*, this CD. [10] Basu A. et al. (2003), *LPS XXXIV*, #1159. [11] Chapman C. (1996), *Meteor. Planet. Sci.*, **31**, 699-725. [12] Clark B.E. et al. (2002), In *Asteroids III* (W. F. Bottke Jr. et al., eds) Univ. of Arizona Press, Tucson, 585-599.